Inorg. Chem. **2002**, *41*, 2738–2746

Synthesis and Structure of Singly Bridged and Doubly Bridged [$MoFe_3S_4$] Double Cubanes with Bidentate Phosphine Ligands

Jaehong Han and Dimitri Coucouvanis*

The Department of Chemistry, The University of Michigan, Ann Arbor, Michigan 48109-1055

Received August 17, 2001

The reactions of the $(Et_4N)_2[(Cl_4\text{-cat})(MeCN)MoFe_3S_4Cl_3]$ (**I**) cluster with $Fe(pp)_2Cl_2$ (pp = depe (bis(1,2-diethylphosphino)ethane) or dmpe (bis(1,2-dimethylphosphino)ethane)) produced the $\{(Cl_4\text{-cat})MoFe_3S_4(pp)_2Cl\}_2(\mu\text{-pp})$ (pp = depe (**III**) or dmpe (**V**)) singly bridged double cubanes. The reactions of **I** with the same bidentate phosphine ligands in the presence of $NaBPh_4$ also produced **III** and the $\{(Cl_4\text{-cat})MoFe_3S_4(dmpe)_2\}_2(\mu\text{-S})(\mu\text{-dmpe})$ (**VI**) doubly bridged double cubane, respectively. The byproduct $(BPh_4)[Fe(dmpe)_2(MeCN)Cl]$ (**VII**) has been isolated from the reaction mixture and crystallographically characterized. The depe analogue of **VI**, $\{(Cl_4\text{-cat})MoFe_3S_4(depe)_2\}_2(\mu\text{-S})(\mu\text{-depe})$ (**IV**), has been successfully prepared from **III** in the presence of excess Li_2S. Similar reactions with $(Et_4N)_2[Fe_4S_4(SPh)_4]$ (**VIII**) have resulted in the formation of the neutral $Fe_4S_4(depe)_2(SPh)_2$ (**IX**) cluster. The chloride analogue of **IX**, $Fe_4S_4(depe)_2Cl_2$ (**XI**), has been obtained by a reaction of **IX** with benzoyl chloride. The crystal and molecular structures of **III**, **VI**, **VII**, and **XI** have been determined by single-crystal X-ray crystallography. The electrochemical and spectroscopic properties, including the Mossbauer spectra of the new clusters, have been determined and analyzed.

Introduction

Attempts to obtain structural models for the nitrogenase cofactor, FeMoco, were initially stimulated by spectroscopic data[1] and later by the X-ray crystal structure determination of the MoFe protein of nitrogenase.[2] Over the years, an impressive amount of Mo/Fe/S chemistry has been generated, and molecules have been obtained that display structural features similar to those of the FeMoco.[3] High-nuclearity clusters with the unusual $MoFe_7S_9$ core of the cofactor have been elusive to synthesis. Many of the available clusters have been synthesized from the $(Et_4N)_2[(Cl_4\text{-cat})(MeCN)MoFe_3S_4Cl_3]$ (**I**) cluster obtained from the reaction between $(Et_4N)_4[(Cl_4\text{-cat})_2Mo_2Fe_6S_8(SEt)_6]$ and PhCOCl.[4] High-nuclearity Mo/Fe/S clusters with the $Mo_2Fe_6S_8$ core, $(Cl_4\text{-cat})_2Mo_2Fe_6S_8(PR_3)_6$ (R = Et, ^{n}Pr, or ^{n}Bu), form by the fusion of **I** following reduction and ligand substitution.[5] The sulfide-voided cuboidal cluster,[6] $(Cl_4\text{-cat})Mo(O)Fe_3S_3(PEt_3)_3(CO)_5$, has also been obtained from the reaction of **I** under high pressure of CO.[7]

Ligand substitution on the Mo site of the $(Et_4N)_2[(Cl_4\text{-cat})(MeCN)MoFe_3S_4Cl_3]$ (**I**) cluster produces various derivatives that show different physical properties.[8,9] The catalytic properties of these compounds in the reduction of N_2H_4 to NH_3, C_2H_2 to C_2H_4, and RN=NR to alkylamine have been reported.[10] The addition of an S^{2-} ligand to the $(Et_4N)_2[(Cl_4\text{-cat})(MeCN)MoFe_3S_4Cl_3]$ (**I**) cluster produced the μ-S bridged $[MoFe_3S_4]$ double cubanes after removing a Cl^- ligand from one of the Fe sites.[8,11−13] These double cubane clusters are

* Author to whom correspondence should be addressed. E-mail: dcouc@umich.edu.

(1) *Nitrogen Fixation*; Müller, A., Newton, W. E., Eds.; Plenum Press: New York, 1983.
(2) Kim, J.; Rees, D. C. *Science* **1992**, *257*, 1677.
(3) *Molybdenum Enzymes*; Spiro, T. G., Ed.; Wiley: New York, 1985.
(4) (a) Cl_4-cat = tetrachlorocatecholate. (b) Palermo, R. E.; Singh, R.; Bashkin, J. K.; Holm, R. H. *J. Am. Chem. Soc.* **1984**, *106*, 2600.
(5) (a) Han, J.; Koutmos, M.; Al-Ahmad, S.; Coucouvanis, D. *Inorg. Chem.* **2001**, *40*, 5985−5999. (b) Demadis, K. D.; Campana, C. F.; Coucouvanis, D. *J. Am. Chem. Soc.* **1995**, *117*, 7832.
(6) (a) Coucouvanis, D.; Han, J.; Moon, N. *J. Am. Chem. Soc.*, submitted for publication, 2001. (b) Tyson, M. A.; Coucouvanis, D. *Inorg. Chem.* **1997**, *36*, 3808.
(7) Han, J.; Coucouvanis, D. *Polyhedron*, submitted for publication.
(8) (a) Demadis, K. D.; Coucouvanis, D. *Inorg. Chem.* **1995**, *34*, 436. (b) Demadis, K. D.; Chen, S. J.; Coucouvanis, D. *Polyhedron* **1994**, *13*, 3147. (c) Coucouvanis, D.; Demadis, K. D.; Kim, C. G.; Dunham, R. W.; Kampf, J. W. *J. Am. Chem. Soc.* **1993**, *115*, 3344.
(9) Mosier, P. E.; Kim, C. G.; Coucouvanis, D. *Inorg. Chem.* **1993**, *32*, 2620.
(10) (a) Malinak, S. M.; Simeonov, A. M.; Mosier, P. E.; McKenna, C. E.; Coucouvanis, D. *J. Am. Chem. Soc.* **1997**, *119*, 1662. (b) Coucouvanis, D. *J. Biol. Inorg. Chem.* **1996**, *1*, 594. (c) Malinak, S. M.; Demadis, K. D.; Coucouvanis, D. *J. Am. Chem. Soc.* **1995**, *117*, 3126. (d) Coucouvanis, D.; Mosier, P. E.; Demadis, K. D.; Patton, S.; Malinak, S. M.; Kim, C. G.; Tyson, M. A. *J. Am. Chem. Soc.* **1993**, *115*, 12193.

10.1021/ic010913+ CCC: $22.00
Published on Web 04/17/2002

often obtained with a ligand bridging the two Mo atoms (N_2H_4, CN^-, S^{2-}, or OH^-) and have a M_8S_9 core with a M/S stoichiometry approaching that of the FeMoco, $MoFe_7S_9$. Clearly, the presence of two Mo atoms and cubane subunits precludes a consideration of these compounds as structural analogues of the FeMoco.

Bridging thiolate ligand substitution by μ-S^{2-} ligands has been reported in the synthesis of other metalloenzymes' active site analogues. For example, the active site of sulfite reductase in *Escherichia coli* consists of an $[Fe_4S_4]$ cluster and siroheme bridged by a cysteinate sulfur atom. A model compound $[Fe_4S_4(LS_3)$-(μ-S)-Fe(OEiBC)$]^{2-}$ has been synthesized by the reaction of [Fe(OEiBC)CI] (OEiBC = dianion of octaethylisobacteriochlorine) and the site-differentiated cluster $[Fe_4S_4(LS_3)(SSiMe_3)]^{2-}$ (LS_3 = trianion of 1,3,5-tris((4,6-dimethyl-3-mercaptophenyl)thio)-2,4,6-tris-(*p*-tolylthio)benzene).[14]

In this paper, we report the synthesis and characterization of the first uncharged bridged $[MoFe_3S_4]^{3+}$ double cubane clusters, $\{(Cl_4\text{-cat})MoFe_3S_4(L)_2Cl\}_2(\mu\text{-L})$ (L = 1,2-depe = diethylphosphinoethane (**III**); L = dmpe = dimethylthylphosphinoethane (**V**))[15] and $\{(Cl_4\text{-cat})MoFe_3S_4(dmpe)_2\}_2(\mu$-S)($\mu$-L) (L = depe (**IV**); dmpe (**VI**)), as well as the mixed ligand, $Fe_4S_4(depe)_2(X)_2$ (X = SPh (**IX**); Cl (**XI**)) clusters.

Experimental Section

All experiments and reactions were carried out under a dinitrogen atmosphere using standard Schlenk line techniques or in an inert atmosphere glovebox. All solvents were distilled under dinitrogen, and nitrogen gas was bubbled through each before its use in the glovebox. Acetonitrile was predried over oven-dried molecular sieves and distilled from CaH_2. Ethyl ether and THF were predried over Na ribbon and further purified by the sodium-benzoketyl method. Dichloromethane was distilled from P_2O_5. PEt_3, depe, and dmpe were purchased from STREM and used for the reaction without further purification. $(Et_4N)_2[(Cl_4\text{-cat})(MeCN)MoFe_3S_4Cl_3]$ (**I**),[4] $(Cl_4\text{-cat})_2Mo_2Fe_6S_8(PEt_3)_6$ (**II**),[5] $(Et_4N)_2[Fe_4S_4Cl_4]$,[16] and $(Et_4N)_2$-$[Fe_4S_4(SPh)_4]$[17] were synthesized according to the published methods.

FT-IR spectra were collected on a Nicolet DX Version 4.56 FT-IR spectrometer in KBr pellets, and the spectra were corrected for background. Elemental analyses were performed by the Microanalytical Laboratory at The University of Michigan. The data were corrected using acetanilide as a standard. Electronic spectra were recorded on a Varian CARY 1E UV−visible spectrometer. Cyclic voltammetry experiments were carried out with an EG&G M260 or K0264 Micro-Cell Kit using a Pt working electrode (vs SCE and 0.1 M $^nBu_4NPF_6$ as supporting electrolyte) under anaerobic conditions. The potentials are reported against Ag/AgCl as a reference electrode. Mössbauer spectra were obtained with the high-sensitivity Mössbauer spectrometer in the Biophysics department at The University of Michigan.[18] All the Mössbauer measurements were carried out at 125 K in zero applied magnetic field. The source was ^{57}Co in a Rh matrix, and the isomer shift was reported versus Fe metal at room temperature. FAB^+ mass spectra were obtained at The University of Michigan Mass Spectroscopy Laboratory with a 3-nitrobenzoyl alcohol matrix.

The numbering scheme used throughout for the complexes is as follows:

$(Et_4N)_2[(Cl_4\text{-cat})Mo(MeCN)Fe_3S_4Cl_3]$	**I**
$(Cl_4\text{-cat})_2Mo_2Fe_6S_8(PEt_3)_6$	**II**
$\{(Cl_4\text{-cat})MoFe_3S_4(depe)_2Cl\}_2(\mu\text{-depe})$	**III**
$\{(Cl_4\text{-cat})MoFe_3S_4(depe)_2\}_2(\mu\text{-S})(\mu\text{-depe})$	**IV**
$\{(Cl_4\text{-cat})MoFe_3S_4(dmpe)_2Cl\}_2(\mu\text{-dmpe})$	**V**
$\{(Cl_4\text{-cat})MoFe_3S_4(dmpe)_2\}_2(\mu\text{-S})(\mu\text{-dmpe})$	**VI**
$(BPh_4)[Fe(dmpe)_2(MeCN)Cl]$	**VII**
$(Et_4N)_2[Fe_4S_4(SPh)_4]$	**VIII**
$Fe_4S_4(depe)_2(SPh)_2$	**IX**
$(Et_4N)_2[Fe_4S_4Cl_4]$	**X**
$Fe_4S_4(depe)_2Cl_2$	**XI**

Synthesis of $\{(Cl_4\text{-cat})MoFe_3S_4(depe)_2Cl\}_2(\mu$-depe) (III), Method A. Compound **I** (1 g, 0.96 mmol) was dissolved in MeCN (30 mL). $Fe(depe)_2Cl_2$ was prepared by dissolving $FeCl_2$ (190 mg, 1.5 mmol) and depe (0.7 mL, 3 mmol) in THF (10 mL). The THF solution was added into the MeCN solution slowly. The reaction mixture formed a black precipitate, and it was stirred overnight. The precipitate was extracted with 60 mL of CH_2Cl_2. Hexane diffusion into this solution resulted in 200 mg of **III** (20% yield) upon standing for 1 day. IR (KBr, cm^{-1}): 2963, 2932, 2875, 1442(s), 1253, 1123, 1025, 974, 763, 625, 521, 408, 352(s). Anal. Calcd for **III** (MW 2377.24): C, 31.32; H, 5.09. Found: C, 31.38; H, 5.06. UV−vis (CH_2Cl_2, nm): 315(sh), 410(sh), 555. FAB^+ (NBA, *m*/*z*): 1087 ($[(Cl_4\text{-cat})MoFe_3S_4(depe)_2Cl]^+$). EPR ($CH_2Cl_2$, 103 K, 1 mW, *g*): 2.09, 1.85.

Method B. Compound **I** (500 mg, 0.48 mmol) and $NaBPh_4$ (500 mg, 1.46 mmol) were dissolved in MeCN (30 mL). After 5 min, depe (0.48 mL, 2 mmol) was added into the reaction mixture dropwise. A black precipitate formed upon standing overnight. The precipitate was isolated and dissolved in CH_2Cl_2. Addition of hexanes afforded 80 mg (16%) of crystalline **III** after standing for 1 day.

Method C. $(Cl_4\text{-cat})_2Mo_2Fe_6S_8(PEt_3)_6$ (**II**) (500 mg, 0.25 mmol) was dissolved in 30 mL of CH_2Cl_2, and an excess of depe (0.48 mL, 2 mmol) was injected through a septum dropwise. Overnight stirring produced 500 mg of **III** in 87% yield. The product showed IR spectra identical to those of the clusters obtained by methods A and B, and its structure was verified by single-crystal X-ray crystallography.

Synthesis of $\{(Cl_4\text{-cat})MoFe_3S_4(depe)_2\}_2(\mu$-S)($\mu$-depe) (IV). $\{(Cl_4\text{-cat})MoFe_3S_4(depe)_2Cl\}_2(\mu$-depe) (**III**) (200 mg, 0.087 mmol) was dissolved in 20 mL of dichloromethane, and excess Li_2S (20 mg, 0.435 mmol) was added to the black solution. The suspension was stirred overnight, and the reaction mixture was filtered to remove the insoluble precipitates (Li_2S and LiCl). Diffusion of hexanes into the reaction filtrate produced 120 mg (0.053 mmol) of a black powder (**IV**) in 60% yield. IR (KBr, cm^{-1}): 2982, 1438-(s), 1255, 1127, 1102, 1030, 781, 744, 707, 603, 481, 459. Anal. Calcd for **IV**·CH_2Cl_2 (MW 2423.45): C, 31.22; H, 5.07. Found:

(11) Challen, P. R.; Koo, S.-M.; Dunham, W. R.; Coucouvanis, D. *J. Am. Chem. Soc.* **1990**, *112*, 2455.
(12) (a) Challen, P. R.; Koo, S. M.; Kim, C. G.; Dunham, R. W.; Coucouvanis, D. *J. Am. Chem. Soc.* **1990**, *112*, 8606. (b) Coucouvanis, D.; Challen, P. R.; Koo, S.-M.; Davis, W. M.; Burtler, W.; Dunham, R. W. *Inorg. Chem.* **1989**, *28*, 4181.
(13) (a) Huang, J.; Holm, R. H. *Inorg. Chem.* **1998**, *37*, 2247. (b) Huang, J.; Mukerjee, S.; Segal, B. M.; Akashi, H.; Zhou, J.; Holm, R. H. *J. Am. Chem. Soc.* **1997**, *119*, 8662.
(14) Zhou, C. Y.; Cai, L. S.; Holm, R. H. *Inorg. Chem.* **1996**, *35*, 2767.
(15) depe = bis(1,2-diethylphosphino)ethane and dmpe = bis(1,2-dimethylphosphino)ethane.
(16) Wong, G. B.; Bobrik, M. A.; Holm, R. H. *Inorg. Chem.* **1978**, *17*, 528.
(17) Averill, B. A.; Herskovitz, T.; Holm, R. H.; Ibers, J. A. *J. Am. Chem. Soc.* **1973**, *95*, 3523.
(18) Moon, N.; Coffin, C. T.; Steinke, D. C.; Sands, R. H.; Dunham, W. R. *Nucl. Instrum. Methods Phys. Res., Sect. B* **1996**, *119*, 555.

C, 30.19; H, 5.29. The CH_2Cl_2 molecule of solvation was detected in the NMR spectrum of **IV**. UV−vis (CH_2Cl_2, nm): 300(sh).

Synthesis of {(Cl$_4$-cat)MoFe$_3$S$_4$(dmpe)$_2$Cl}$_2$(μ-dmpe) (V). Compound **V** was synthesized in 85% yield by using method A for **III**. IR (KBr, cm^{-1}): 2975, 2946, 2931, 2905, 1441(s), 1420, 1254, 939, 708, 648, 526, 462, 407. NMR (DMSO-d_6, 400 MHz, ppm): 3.36 (4H, Mo−P−CH_2), 3.16 (12H, Mo−P−CH_3), 2.16 (4H, Fe_A−P−CH_2), 2.08 (4H, Fe_A−P−CH_2), 1.42 (6H, Fe_B−P−CH_3), 1.40 (4H, Fe_B−P−CH_2), 1.38 (10H, Fe_A−P−CH_3, Fe_B−P−CH_2), 1.12 (36H, Fe_A−P−CH_3, Fe_B−P−CH_3). Peak assignment was helped by two-dimensional (gCOSY) experiment. UV−vis (CH_2Cl_2, nm): 464, 555(sh).

Synthesis of {(Cl$_4$-cat)MoFe$_3$S$_4$(dmpe)$_2$}$_2$(μ-S)(μ-dmpe) (VI). **VI** was obtained from **V** in CH_2Cl_2, as a black powder in 65% yield, using the same method used in the synthesis of **IV**. When method B (as used for **III**) was used in MeCN, black rhombic crystalline **VI** was isolated from the CH_2Cl_2 extract in 25% yield. IR (KBr, cm^{-1}): 2972, 2920, 2902, 1441(s), 1389, 1254, 934, 804, 780, 653, 517, 352, 347(sh), 302. Anal. Calcd for **VI**·$^3/_2$Hex (MW 2187.249): C, 28.01; H, 4.65. Found: C, 28.20; H, 4.23. FAB$^+$ (NBA, *m*/*z*): 974 ([{(Cl$_4$-cat)MoFe$_3$S$_4$(dmpe)$_2$SH} + H]$^+$).

Purple crystalline (BPh_4)[Fe(dmpe)$_2$(MeCN)Cl] (**VII**) was also isolated from the MeCN reaction filtrate of **VI** after ether addition. IR (KBr, cm^{-1}): 3055, 2916(s), ν(C≡N) for 2245(w), 1077(s), 840-(s), 401, 378(s), 352(s), 345. The X-ray powder pattern of this compound was found to be identical to that calculated from the structure obtained from single-crystal X-ray diffraction data.

Synthesis of Fe$_4$S$_4$(depe)$_2$(SPh)$_2$ (IX). Compound **VIII** (640 mg, 0.5 mmol) and $NaBPh_4$ (500 mg, 1.5 mmol) were dissolved into 30 mL of MeCN. As the solution was stirred, depe (0.24 mL, 1.0 mmol) was added. The reaction mixture was stirred for 17 h. The precipitate was extracted with 50 mL of CH_2Cl_2. Crystallization of the product was affected following the addition of hexane into the solution. A needle-shaped crystalline product was obtained (200 mg, 43% yield). IR (KBr, cm^{-1}): 3057, 3047, 2968, 2933, 2902, 2875, 1471(s), 1454(s), 1125(s), 762(s), 476(s), 429, 423, 364(s). ^{1}H-NMR (300 MHz, CD_2Cl_2): 9.16 (2H, br s, Ph), 7.20 (6H, br.s, Ph), 5.98 (2H, br.s, Ph). FAB$^+$-MS (NBA, *m*/*z*): only a fragment of [Fe$_4$S$_4$(depe)$_2$] was observed. The stoichiometry of this compound was established by ^{1}H-NMR spectroscopy and microprobe analysis for Fe, S, and P (relative ratio for Fe:S:P = 4:5.8:3.9). The compound was EPR silent in frozen DMF solution at 20 K.

Synthesis of Fe$_4$S$_4$(depe)$_2$Cl$_2$ (XI). Fe$_4$S$_4$(depe)$_2$(SPh)$_2$ (**VIII**) (460 mg, 0.5 mmol) was dissolved in 25 mL of CH_2Cl_2, and PhCOCl (0.12 mL, 1 mmol) was added dropwise. The reaction mixture was stirred for 3 h and layered with 20 mL of hexanes. A black crystalline material as well as powder deposited on the bottom of flask after 1 day. The filtered product mixture was extracted with 50 mL of THF, and only the crystalline material was soluble. Ether (75 mL) diffusion into THF extract gave black rod-shaped crystals (100 mg, 0.12 mmol) in 24% yield after 1 day. The compound was EPR silent in frozen DMF solution at 20 K. The X-ray powder pattern of this compound was found to be identical to that calculated from the structure obtained from single-crystal X-ray diffraction data.

X-ray Crystallography. All diffraction data, except those for {(Cl$_4$-cat)MoFe$_3$S$_4$(depe)$_2$Cl}$_2$(μ-depe) (**III**) and (BPh_4)[Fe(dmpe)$_2$-(MeCN)Cl] (**VII**), were collected at 158(2) K using a Siemens SMART area diffractometer. Data sets for **III** and **VII** were collected at room temperature using a P3-F four-circle diffractometer. Appropriate crystals of **III**, for single-crystal X-ray crystallography, were grown by vapor diffusion of hexanes into a CH_2Cl_2 solution of the compound. A black rhombic-shaped crystal (0.30 × 0.30 × 0.20 mm) was chosen and mounted under an Ar atmosphere in a quartz capillary (Charles Supper Co.) on a P3-F diffractometer. Unit cell parameters were determined from 20 machine-centered reflections, and three standard reflections examined after every 97th measurement showed no detectable crystal decay over the data collection period. Axial rotation photographs and systematic absences unambiguously established the space group in the orthorhombic system as *Pbca*. A single crystal of **VII** was isolated by filtration of the mother liquor (ether/MeCN). Data collection for **VII** was carried out under the same experimental conditions as for **III**. Crystalline Fe$_4$S$_4$(depe)$_2$(SPh)$_2$ (**IX**) for single-crystal X-ray crystallography was obtained by hexane diffusion into a CH_2Cl_2 solution of **IX**, but the crystals gave poor quality diffraction data. A monoclinic *P* lattice was obtained a cell with values of $a = 16.3610(1)$ Å, $b = 11.8274(2)$ Å, $c = 22.8002(2)$ Å, and $\beta = 110.762(1)°$. All the non-hydrogen atoms were refined, and the final *R* factor was around 0.23 after refinement. Due to the poor quality of the structural refinement, it is not reported in detail herein. Nevertheless, atomic connectivity in **IX** is the same as that in **XI** (vide infra). Crystalline Fe$_4$S$_4$(depe)$_2$Cl$_2$ (**XI**) for single-crystal X-ray crystallography was obtained by ether diffusion over a THF solution of this cluster.

Hydrogen atoms were added at their calculated positions for all the reported structures. No H atoms were added to the disordered solvent's molecules.

The crystal data and structural parameters for **III**, **VI**, **VII**, and **XI** are shown in Table 1. The structures for the compounds were solved by direct methods to locate heavy atoms, and the non-hydrogen atoms were located through subsequent difference Fourier syntheses. Structural refinement was carried out by full-matrix least-squares on F^2. All non-hydrogen atoms were refined with anisotropic thermal parameters, and all hydrogen atoms were refined isotropically except those on disordered carbon atoms. All calculations were performed using SHELXTL-NT version 5.1 software.

Results and Discussion

Ligand substitution reactions at the labile Mo site in the (Et_4N)$_2$[(Cl$_4$-cat)(MeCN)MoFe$_3$S$_4$Cl$_3$] (**I**) cluster have been studied extensively with various unidentate ligands.[4] The substitution of the Cl$_4$-cat ligand with polycarboxylate ligands has also been reported.[8] Ligand substitutions at the Fe sites of the (Et_4N)$_2$[(Cl$_4$-cat)(MeCN)MoFe$_3$S$_4$Cl$_3$] (**I**) cluster are not as common and have been limited to RS^- and X^-. To our knowledge, bidentate phosphine ligand introduction into **I** by ligand substitution has not been reported previously.

The reaction between **I** and bidentate phosphine ligands gave neutral double cubane clusters containing the [MoFe$_3$S$_4$]$^{3+}$ cores (**III**−**VI**). A similar result is obtained in the reaction between the (Et_4N)$_2$[Fe$_4$S$_4$(SPh)$_4$] (**VIII**) cluster and depe,[15] which results in the uncharged [Fe$_4$S$_4$]$^{2+}$ single cubane, Fe$_4$S$_4$-(depe)$_2$(SPh)$_2$ (**IX**). The reaction between the (Et_4N)$_2$[Fe$_4$S$_4$-Cl$_4$] cluster (**X**) and monodentate PR_3 is known to produce [Fe$_4$S$_4$]$^+$ as well as the more reduced clusters [Fe$_4$S$_4$]^0, [Fe$_8$S$_8$]^0, or [Fe$_4$S$_4$]$_n^0$.[19] Similarly, reactions of **I** with monodentate phosphines give reduced clusters with the [Mo$_2$-Fe$_6$S$_8$]$^{4+}$ cores.[5b] The origin of this difference in cluster product formation, as a consequence of monodentate vs

(19) (a) Tyson, M. A.; Demadis, K. D.; Coucouvanis, D. *Inorg. Chem.* **1995**, *34*, 4519. (b) Goh, C.; Segal, B. M.; Huang, J. S.; Long, J. R.; Holm, R. H. *J. Am. Chem. Soc.* **1996**, *118*, 11844.

Table 1. Crystal Data and Structure Refinements for {(Cl$_4$-cat)MoFe$_3$S$_4$(depe)$_2$Cl}$_2$(μ-depe) (**III**), {(Cl$_4$-cat)MoFe$_3$S$_4$(dmpe)$_2$}$_2$(μ-S)(μ-dmpe) (**VI**), (BPh$_4$)[Fe(dmpe)$_2$(MeCN)] (**VII**), and Fe$_4$S$_4$(depe)$_2$Cl$_2$ (**XI**)

	III	VI	VII	XI
empirical formula	$C_{62}H_{120}Cl_{10}Fe_6Mo_2O_4P_{10}S_8$	$C_{55}H_{105}Cl_{22}Fe_6Mo_2O_4P_{10}S_9$	$C_{38}H_{55}BClFeNP_4$	$C_{20}H_{45}Cl_2Fe_4P_4S_4$
formula weight	2377.24	2735.51	751.82	831.98
temp, K	293(2)	158(2)	293(2)	158(2)
wavelength, Å	0.71073	0.71073	0.71073	0.71073
cryst syst	orthorhombic	orthorhombic	monoclinic	monoclinic
space group	*Pbca*	*Pbca*	*P*2(1)/*c*	*P*2(1)/*n*
unit cell dimensions, Å and deg	$a = 23.420(5)$ $b = 17.376(4)$ $c = 23.773(5)$	$a = 25.5705(3)$ $b = 24.9521(3)$ $c = 32.8954(4)$	$a = 14.781(3)$ $b = 14.847(3)$ $c = 18.490(4)$ $\beta = 94.75(3)$	$a = 13.85750(10)$ $b = 15.0055(2)$ $c = 17.01310(10)$ $\beta = 105.3810(10)$
vol, Å^3	9674(3)	20988.5(4)	4043.6(14)	3410.97(6)
Z, calculated density, mg/m^3	4, 1.632	8, 1.731	4, 1.235	4, 1.620
absorption coefficient, mm^{-1}	1.778	1.966	0.624	2.268
F(000)	4848	11000	1592	1708
cryst size, mm	0.30 × 0.30 × 0.20	0.16 × 0.24 × 0.36	0.3 × 0.2 × 0.2	0.18 × 0.20 × 0.20
θ range for data collection, deg	1.92−22.55	2.05−2946	1.95−22.54	2.48−26.39
limiting indices	$0 \le h \le 25$ $0 \le k \le 18$ $-25 \le l \le 0$	$-34 \le h \le 33$ $-34 \le k \le 33$ $-45 \le l \le 44$	$0 \le h \le 15$ $0 \le k \le 12$ $-15 \le l \le 15$	$-17 \le h \le 17$ $-18 \le k \le 18$ $-21 \le l \le 21$
reflections collected/unique	6355/6354	207708/27411	2894/2749	30875/6979
R(int)	0.6328	0.1321	0.0238	0.0492
completeness to θ, %	99.8	94.1	51.7	99.8
data/restraints/params	6354/0/420	27411/0/1003	2749/0/416	6979/0/306
GOF on F^2	0.945	1.169	1.624	1.092
final *R* indices [$I > 2\sigma(I)$]	R1 = 0.0810, wR2 = 0.1664	R1 = 0.1188, wR2 = 0.2121	R1 = 0.1042, wR2 = 0.3264	R1 = 0.0340, wR2 = 0.0603
R indices (all data)	R1 = 0.1838, wR2 = 0.2092	R1 = 0.1736, wR2 = 0.2347	R1 = 0.1160, wR2 = 0.3432	R1 = 0.0543, wR2 = 0.0663

bidentate phosphine ligands usage, is not clear, but it may be due to the different electronic properties and/or steric characteristics of the ligands.

The {(Cl$_4$-cat)MoFe$_3$S$_4$(depe)$_2$Cl}$_2$(μ-depe) (**III**) cluster can also be synthesized from (Cl$_4$-cat)$_2$Mo$_2$Fe$_6$S$_8$(PEt$_3$)$_6$ (**II**) upon addition of an excess of depe in CH_2Cl_2 solution. The edge-fused double cubane, **II**, undergoes oxidative cleavage as depe is substituted for PEt$_3$ and forms the oxidized {(Cl$_4$-cat)MoFe$_3$S$_4$(depe)$_2$Cl}$_2$(μ-depe) (**III**) cluster product. Since external chloride was not introduced, the chloride ligands on the Fe atom in the {(Cl$_4$-cat)MoFe$_3$S$_4$(depe)$_2$Cl}$_2$-(μ-depe) (**III**) cluster must have been obtained from CH_2Cl_2, which was apparently reduced to Cl^- and H_2ClC^-. Unlike the depe compounds, {(Cl$_4$-cat)MoFe$_3$S$_4$(depe)$_2$Cl}$_2$-(μ-depe) (**III**) and {(Cl$_4$-cat)MoFe$_3$S$_4$(depe)$_2$}$_2$(μ-S)(μ-depe) (**IV**), the {(Cl$_4$-cat)MoFe$_3$S$_4$(dmpe)$_2$}$_2$(μ-S)(μ-dmpe) cluster (**VI**) was not as soluble in CH_2Cl_2, THF, or MeCN. The synthesis of **VI** was achieved by the reaction between Li_2S in DMF and the {(Cl$_4$-cat)MoFe$_3$S$_4$(dmpe)$_2$Cl}$_2$(μ-dmpe) cluster (**V**), obtained from the reaction of **I** with Fe-(dmpe)$_2$Cl$_2$. The isolated product, **VI**, was sparingly soluble in DMF.

When the **I**/dmpe/NaBPh$_4$ procedure was followed, **VI** was the only isolable product, and (BPh$_4$)[Fe(MeCN)(dmpe)$_2$Cl] (**VII**) was isolated as a reaction byproduct. In this reaction, the S^{2-} ligand, which is necessary for the formation of **VI**, is probably obtained from degradation of **I**. Synthesis of **VI** by the **I**/dmpe/NaBPh$_4$ procedure is preferable, but the product **VI** was always contaminated by an unknown byproduct. Successive recrystallization from DMF gave spectroscopically pure **VI**, which was quite insoluble in most solvents.

The reaction of the (Et$_4$N)$_2$[Fe$_4$S$_4$(SPh)$_4$] (**VIII**) cluster with depe in the presence of NaBPh$_4$ produced the neutral

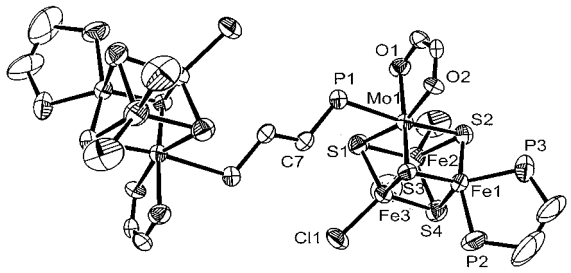

Figure 1. Crystallographic structure of the {(Cl$_4$-cat)MoFe$_3$S$_4$(depe)$_2$Cl}$_2$-(μ-depe) (**III**) cluster.

Fe$_4$S$_4$(depe)$_2$(SPh)$_2$ (**IX**) cluster. The reaction of (Et$_4$N)$_2$-[Fe$_4$S$_4$Cl$_4$] (**X**) with depe in the presence of NaBPh$_4$ did not produce the expected Fe$_4$S$_4$(depe)$_2$Cl$_2$ (**XI**) product. The latter could only be obtained by the reaction of Fe$_4$S$_4$(depe)$_2$(SPh)$_2$ with benzoyl chloride.

Structural Descriptions. Among the double cubane clusters reported in this paper, {(Cl$_4$-cat)MoFe$_3$S$_4$(depe)$_2$Cl}$_2$-(μ-depe) (**III**) and {(Cl$_4$-cat)MoFe$_3$S$_4$(dmpe)$_2$}$_2$(μ-S)(μ-dmpe) (**VI**) have been crystallized and their structures determined and shown in Figures 1 and 2. The structure of **III** has a crystallographic *C*2 rotation axis going through the center of the CH_2-CH_2 bond of the μ-depe ligand. The general features of the MoFe$_3$S$_4$ units of compounds **III** and **VI** are similar to those of other μ_2-S bridged MoFe$_3$S$_4$ double cubane clusters except that most of the bonds are shortened. This type of bond shrinkage was observed also for the uncharged (Cl$_4$-cat)Mo(PEt$_3$)Fe$_3$S$_4$(SPEt$_3$)$_2$Cl cluster, and the possible manifestation of the charge effect on the bond distances has been discussed.[7]

Each [MoFe$_3$S$_4$]$^{3+}$ subunit in the {(Cl$_4$-cat)MoFe$_3$S$_4$(depe)$_2$-Cl}$_2$(μ-depe) (**III**) cluster is connected by a μ-depe bridging

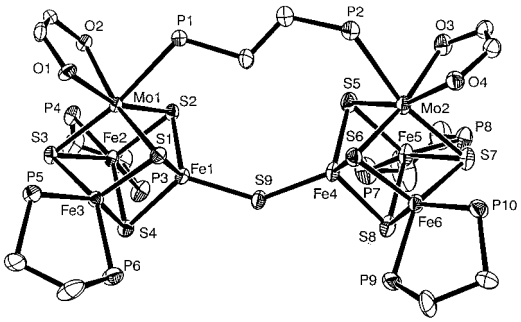

Figure 2. Crystallographic structure of the $\{(Cl_4\text{-cat})MoFe_3S_4(dmpe)_2\}_2$-($\mu$-S)($\mu$-dmpe) (**VI**) cluster.

ligand, and the distance between the Mo(1) and Mo(1)# atoms is 8.768(2) Å. The coordination geometry of the Mo(1) atom in **III** is distorted octahedral with the Mo coordinated by three inorganic μ_3-sulfur atoms (Mo(1)−S(1), 2.319(4) Å; Mo(1)−S(2), 2.341(4) Å; Mo(1)−S(3), 2.320(4) Å), two oxygen atoms from $Cl_4\text{-cat}^{2-}$ (Mo(1)−O(1), 2.120(9) Å; Mo(1)−O(2), 2.124(9) Å), and a phosphorus atom from μ-depe (Mo(1)−P(1), 2.597(4) Å). The distance of the corresponding Mo−P bond in the $(Cl_4\text{-cat})_2Mo_2Fe_6S_8(PEt_3)_6$ cluster (**II**) is 2.601(4) Å. The Fe(3) atom with a chloride terminal ligand (Fe(3)−Cl(1), 2.221(5) Å) has the usual tetrahedral coordination geometry with three μ_3-sulfur ligands (Fe(3)−S(1), 2.259(5) Å; Fe(3)−S(3), 2.244(4) Å; Fe(3)−S(4), 2.216(5) Å). The other two Fe atoms in the $[MoFe_3S_4]^{3+}$ cluster of **III** have five-coordinated distorted trigonal bipyramidal geometry as a result of bidentate depe ligand coordination to the Fe atoms. For the Fe(1) atom, one of μ_3-sulfur atoms (Fe(1)−S(2), 2.248(5) Å) and one of the phosphorus atoms (Fe(1)−P(2), 2.268(6) Å) are ligated to the Fe atom as axial ligands, and the rest of the ligands are equatorially coordinated (Fe(1)−S(3), 2.174(4) Å; Fe(1)−S(4), 2.214(5) Å; Fe(1)−P(3), 2.244(5) Å). The Fe(2) atom also has the same coordination geometry with two axial ligands (Fe(2)−S(2), 2.245(5) Å; Fe(2)−P(5), 2.237(7) Å) and three equatorial ligands (Fe(2)−S(1), 2.168(5) Å; Fe(2)−S(4), 2.214(5) Å; Fe(2)−P(4), 2.229(7) Å). The equatorial bonds Fe(1)−S(3) and Fe(2)−S(1) at 2.174(4) and 2.168(5) Å, respectively, are very short compared to other intracuboidal Fe−S distances. The average distance of other Fe−S bonds in the $[MoFe_3S_4]^{3+}$ core of **III** is 2.234(5) Å.

The average Mo−Fe distance in the $\{(Cl_4\text{-cat})MoFe_3S_4(depe)_2Cl\}_2$($\mu$-depe) (**III**) cluster is 2.73(3) Å. The distance from Mo(1) to the tetrahedral Fe(3) atoms (2.662(2) Å) is significantly shorter than those from the Mo(1) to the trigonal bipyramidal Fe centers. The three Fe atoms in **III** form an isosceles triangle. Two Fe−Fe pairs, Fe(1)−Fe(3) and Fe(2)−Fe(3), have short distances of 2.622(2) and 2.629(2) Å, respectively. The Fe(1)−Fe(2) distance is 3.190(3) Å. The average Fe−Fe distance in the $(Et_4N)_2[(Cl_4\text{-cat})Mo(MeCN)Fe_3S_4Cl_3]$ (**I**) cluster and in the reduced $[MoFe_3S_4]^{2+}$ core of the $(Cl_4\text{-cat})_2Mo_2Fe_6S_8(PEt_3)_6$ (**II**) cluster is 2.733(5) and 2.639(3) Å, respectively. This type of Fe−Fe bond distance distribution is found in the Mo/Fe/S clusters with the $[MoFe_3S_3]^{2+,4+}$ core.[20] The larger Fe−Fe distances often are found between Fe atoms with the greatest coordination numbers. At present, it is difficult to establish the relative importance of electronic versus steric (coordination sphere crowding) reasons for these differences in the Fe−Fe distances.

Table 2. Selected Bond Distances of the $\{(Cl_4\text{-cat})MoFe_3S_4(depe)_2Cl\}_2$($\mu$-depe) (**III**) and $\{(Cl_4\text{-cat})MoFe_3S_4(dmpe)_2\}_2$($\mu$-S)($\mu$-dmpe) (**VI**) Clusters[a]

bond	III	VI-A	VI-B
Mo(1)−Mo(1)#	8.768(2)	7.5974(10)	
Mo(1)−P(1)	2.597(4)	2.561(2)	2.608(3)
Mo(1)−O(1)	2.120(9)	2.121(6)	2.135(7)
Mo(1)−O(2)	2.124(9)	2.119(6)	2.122(6)
Mo(1)−S(1)	2.319(4)	2.362(2)	2.333(2)
Mo(1)−S(2)	2.341(4)	2.383(2)	2.354(3)
Mo(1)−S(3)	2.320(4)	2.363(2)	2.366(2)
Fe(1)−S(2)	2.248(5)	2.240(2)	2.246(3)
Fe(1)−P(2)	2.268(6)	2.237(3)	2.233(3)
Fe(1)−S(3)	2.174(4)	2.196(3)	2.186(3)
Fe(1)−S(4)	2.214(5)	2.251(3)	2.239(3)
Fe(1)−P(3)	2.244(5)	2.257(3)	2.254(3)
Fe(2)−S(2)	2.245(5)	2.251(3)	2.263(3)
Fe(2)−P(5)	2.237(7)	2.243(3)	2.240(3)
Fe(2)−S(1)	2.168(5)	2.185(3)	2.209(3)
Fe(2)−S(4)	2.214(5)	2.247(3)	2.241(3)
Fe(2)−P(4)	2.229(7)	2.244(3)	2.238(3)
Fe(3)−S(1)	2.259(5)	2.242(2)	2.277(3)
Fe(3)−S(3)	2.244(4)	2.233(3)	2.236(3)
Fe(3)−S(4)	2.216(5)	2.240(3)	2.235(3)
Fe(3)−Cl(1)	2.221(5)	2.158(3)	2.177(3)
Mo(1)−Fe(2)	2.765(2)	2.7157(14)	2.7123(16)
Mo(1)−Fe(2)	2.766(3)	2.7026(15)	2.7481(16)
Mo(1)−Fe(3)	2.662(2)	2.6806(14)	2.7228(16)
Fe(1)−Fe(3)	2.622(2)	2.6579(17)	2.6372(18)
Fe(2)−Fe(3)	2.629(3)	2.6550(18)	2.6240(19)
Fe(1)−Fe(2)	3.190(3)	3.187(2)	3.187(2)

[a] See Figures 1 and 2.

The $[MoFe_3S_4]^{3+}$ subunits in the $\{(Cl_4\text{-cat})MoFe_3S_4(dmpe)_2\}_2$($\mu$-S)($\mu$-dmpe) (**VI**) cluster are connected by μ-dmpe and μ-S bridging ligands (Figure 2). The distance between Mo(1) and Mo(2) is 7.5974(10) Å, and the distance between Fe(1) and Fe(4), connected through μ-S(9), is 4.0503(18) Å. This distance is longer than the Fe-μ-S−Fe distance (3.433(4) Å) in the $[(Fe_4S_4Cl_4)_2(\mu\text{-S})]^{4-}$ cluster.[11] The angle of the bridging S^{2-} ligand in compound **VI** is exceptionally large (138.26(13)°), and is much larger than that of 104.1° found in the $[\{(C_2O_4)MoFe_3S_4Cl_2\}_2(\mu\text{-S})(\mu\text{-CN})]^{5-}$ cluster.[8a] The same angle in the $[(Fe_4S_4Cl_4)_2(\mu\text{-S})]^{4-}$ cluster is 102.2°.[11] The long P−CH_2CH_2−P bridge in **VI** is very likely the reason for the obtuse Fe−S−Fe angle. The intercuboidal Fe−S distances for Fe(1)−S(9) and Fe(4)−S(9) are 2.158(3) and 2.177(3) Å, respectively. The average intracuboidal Fe−S distances for Fe(1) and Fe(4) are 2.238(3) and 2.250(14) Å, respectively. A structural comparison of the doubly bridged $[MoFe_3S_4]$ double cubanes is shown in Table 2. Coordination geometries of the metal centers in **VI** are similar to those in **III**. Two Mo atoms form a distorted octahedral coordination geometry by the same ligand atoms (two oxygen, one phosphorus, and three μ_3-sulfur atoms). The Fe atoms (Fe(2), Fe(3), and Fe(6)) bound to dmpe ligands show a distorted square pyramidal coordination geometry with short distances of axially coordinated μ_3-S ligands (Fe(2)−S(2), 2.196(3) Å; Fe(3)−S(1), 2.185(3) Å;

(20) Coucouvanis, D.; Han, J.; Moon, N. Submitted for publication.

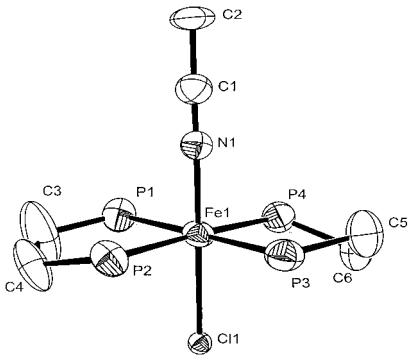

Figure 3. Crystallographic structure of the $(BPh_4)[Fe(dmpe)_2(MeCN)]$ (**VII**) cluster. Selected bond distances (Å) and angles (deg): Fe(1)−P(1), 2.232(5); Fe(1)−P(2), 2.240(4); Fe(1)−P(3), 2.250(5); Fe(1)−P(4), 2.242(5); av Fe−P, 2.241(4); Fe(1)−Cl(1), 2.445(3); Fe(1)−N(1), 1.886(14); Cl(1)−Fe(1)−N(1), 1775(4); P(1)−Fe(1)−P(2), 83.69(17); P(3)−Fe(1)−P(4), 85.42(18); av N−Fe−P, 90.7(6); av Cl−Fe−P, 89.3(8).

Fe(6)−S(6), 2.186(3) Å). The average Fe−S distance between the square pyramidal Fe atoms (Fe(2), Fe(3), and Fe(6)) and their axial S ligand in **VI** is 2.189(4) Å. The Fe(5) atom uniquely shows a five-coordinate distorted trigonal bipyramidal geometry similar to those found in **III** (Fe(1) and Fe(2)). The S(7) and the P(7) atoms are axial ligands for Fe(5) at a distance of 2.263(3) and 2.240(3) Å, respectively. The other three ligands, S(5), S(8), and P(8), define the trigonal plane (Fe(5)−S(5), 2.209(3) Å; Fe(5)−S(8), 2.241(3) Å; Fe(5)−P(8), 2.238(3) Å). The average Mo(1)−Fe(1,2,3) distance is 2.700(10) Å, and that of Mo(2)−Fe(4,5,6) is 2.728(11) Å. Three Fe atoms in each $[MoFe_3S_4]^{3+}$ subunit of **VI** also form an isosceles triangle. The Fe(1)−Fe(2) and Fe(1)−Fe(3) distances in one of the cubane subunits in **VI** are 2.658(2) and 2.655(2) Å, respectively. The Fe(4)−Fe(5) and Fe(4)−Fe(6) distances in the other subunit of **VI** are 2.624(2) and 2.637(2) Å, respectively. The long Fe−Fe distances (Fe(4)−Fe(5) and Fe(4)−Fe(6)) in the two $[MoFe_3S_4]^{3+}$ units are both 3.187(2) Å.

The $(BPh_4)[Fe(dmpe)_2(MeCN)Cl]$ (**VII**) is a hexacoordinate octahedral Fe monomer with two bidentate phosphine ligands (Figure 3). There are many structurally characterized Fe complexes with the same coordination geometry of bidentate phosphine ligands.[21] Selected distances of these complexes with common $FeX_2(pp)_2$ units (X = Cl, H, N_2, CCPh, C=CHPh; pp = dmpe, depe) are compared to those in **VII** (Table 3). In **VII**, the N(1) atom of the MeCN and chloride ligands are axially bound at distances of 1.886(14) and 2.445(3) Å, respectively. The Fe(1)−N(1) bond is within the range of 1.784(9)−1.897(3) Å, found for other Fe−dmpe complexes with N_2 or C≡CPh axial ligands. When the alkenyl ligand (C=CHPh) binds on the Fe of the $FeCl(dmpe)_2$ unit, the Fe−C distance is 1.750(7) Å. The Fe(1)−Cl distance in **VII** is the longest among the related compounds (Table 3). The distance of the Fe−Cl bond in the $FeClX(pp)_2$ complexes is well-known to be insensitive to the change of X.[22] The average Fe−P distance of **VII** is 2.241(5) Å. Due to the absence of the structural data regarding the $FeX(MeCN)(pp)_2$ complex, Fe(1)−N(1) and N(1)−C(1) bonds in **VII** were compared to those in the other related compounds, $[Fe(MeCN)_4(PEt_3)_2]^{2+}$ and **I**. The $[Fe(MeCN)_4(PEt_3)_2](BPh_4)_2$ monomer has been synthesized, and its structure has been reported by us.[5a] The average Fe−N distance of 1.916(3) Å in the $[Fe(MeCN)_4(PEt_3)_2]^{2+}$ molecule is close to the Fe(1)−N(1) distance of 1.886(14) Å in **VII**. The latter is also similar to that of 1.908(8) Å in the $[Fe(NCNEt_2)_2(depe)_2](BF_4)_2$ complex.[21h] The labile MeCN ligand on the Mo site of **I** has a N≡C bond at a distance of 1.13(3) Å.[5a] The latter is comparable to the distance of 1.154 Å for N(1)−C(1) in **VII** and to 1.14(1) Å in the $[Fe(NCNEt_2)_2(depe)_2](BF_4)_2$ complex.

The uncharged $Fe_4S_4(depe)_2Cl_2$ (**XI**) cluster has two different types of terminal ligands, Cl^- and depe (Figure 4). A site-differentiated $[Fe_4S_4Cl_2(Et_2dtc)_2]^{2-}$ single cubane, with bidentate ligands on two of the Fe atoms, has been reported previously.[23] The compound was synthesized by the ligand substitution of either Cl^- in the $[Fe_4S_4Cl_4]^{2-}$ cluster by dtc^- or SPh^- in the $[Fe_4S_4(SPh)_2(Et_2dtc)_2]^{2-}$ cluster in a reaction with benzoyl chloride. The Fe atoms with a chloride terminal ligand in **XI** have tetrahedral coordination geometry. The Fe(1) atom has a Cl(1) terminal ligand (Fe(1)−Cl(1), 2.2252(9) Å) and three μ_3-S ligands (Fe(1)−S(2), 2.2899(9) Å; Fe(1)−S(3), 2.2806(9) Å; Fe(1)−S(4), 2.2810(8) Å). The Fe(2) atom has Cl(2), S(1), S(3), and S(4) ligands at distances of 2.2447(9), 2.3054(9), 2.2946(8), and 2.2918(9) Å, respectively. The average Fe−Cl distance of 2.24(1) Å is a little longer than that of 2.216(2) Å in the $(Et_4N)_2[Fe_4S_4Cl_4]$ cluster.[24] The Fe(1)−Fe(2) distance of 2.6710(6) Å is very short. The corresponding distance in the $[Fe_4S_4Cl_2(Et_2dtc)_2]^{2-}$ cluster is found at 2.766(3) Å. The Fe(3)−Fe(4) distance in **XI** is 2.9050(6) Å, and the corresponding distance in $[Fe_4S_4Cl_2(Et_2dtc)_2]^{2-}$ is 3.045(4) Å. The average Fe−Fe distance in the $(Et_4N)_2[Fe_4S_4Cl_4]$ cluster is 2.766(5) Å.[24] The Fe(3) and the Fe(4) atoms with depe ligands have the same pentacoordinate distorted square pyramidal coordination geometry. The S(4) atom is ligated to the Fe(3) atom as an axial ligand at a distance of 2.2859(8) Å, and the S(1), S(2), P(1), and P(2) atoms are bound to Fe(3) as equatorial ligands at distances of 2.2624(9), 2.2606(8), 2.2877(8), and 2.2592(9) Å, respectively. For the Fe(4) atom, the S(3), S(1), S(2), P(3), and P(4) atoms are found as axial and equatorial ligands at distances of 2.2856(8), 2.2692(8), 2.2522(9), 2.2544(9), and 2.2660(9) Å, respectively. The average Fe−P distance

(21) (a) Hughes, D. L.; Leigh, G. J.; Jimenez-Tenorio, M.; Rowley, A. T. *J. Chem. Soc., Dalton Trans.* **1993**, 75. (b) Field, L. D.; George, A. V.; Hambley, T. W. *Inorg. Chem.* **1990**, *29*, 4565. (c) Hills, A.; Hughes, D. L.; Jimenez-Tenorio, M.; Leigh, G. J. *J. Organomet. Chem.* **1990**, *391*, C41. (d) Baker, M. V.; Field, L. D.; Hambley, T. W. *Inorg. Chem.* **1988**, *27*, 2872. (e) Wiesler, B. E.; Tuczek, F.; Näther, C.; Bensch. W. *Acta Crystallogr., Sect. C* **1998**, *54*, 44. (f) Buys, I. E.; Field, L. D.; Hambley, T. W.; McQueen, A. E. D. *Acta Crystallogr., Sect. C* **1993**, *49*, 1056. (g) Wiesler, B. E.; Lehnert, N.; Tuczek, F.; Neuhausen, J.; Tremel, W. *Angew. Chem., Int. Ed.* **1998**, *37*, 815. (h) Martins, L. M. D. R. S.; Fraústo da Silva, J. J. R.; Pombeiro, A. J. L.; Henderson, R. A.; Evans, D. J.; Benetollo, F.; Bombieri, G.; Michelin, R. A. *Inorg. Chim. Acta* **1999**, *291*, 39.

(22) Di Vaira, M.; Midollini, S.; Sacconi, L. *Inorg. Chem.* **1981**, *20*, 3430.

(23) (a) Kanatzidis, M. G.; Coucouvanis, D.; Simopoulos, A.; Kostikas, A.; Papaefthymiou, V. *J. Am. Chem. Soc.* **1985**, *107*, 4925. (b) Kanatzidis, M. G.; Ryan, M.; Coucouvanis, D.; Simopoulos, A.; Kostikas, A. *Inorg. Chem.* **1983**, *22*, 179.

(24) Bobrik, M. A.; Hodgson, K. O.; Holm, R. H. *Inorg. Chem.* **1977**, *16*, 1851.

Table 3. Comparisons of Selected Bond Distances and IR Stretching Frequencies of $(BPh_4)[Fe(dmpe)_2(MeCN)]$ (**VII**) and Related Compounds

compound	av Fe−P	Fe−Cl (H)	Fe−C (N)	NN, CN, CC	ν(NN, CN, CC), cm^{-1}	reference
[FeCl(MeCN)(dmpe)$_2$](BPh4) (**VII**)	2.241(4)	2.445(3)	1.886(14) (N)	1.154(18) (NC)	2245	this work
$FeCl^2(dmpe)_2$	2.236	2.351(1)				22
[FeCl(C═CHPh)(dmpe)$_2$]I	2.261(3)	2.355(2)	1.750(7)	1.268(11) (C═C)	1615	21a
FeCl(CCPh)(dmpe)$_2$	2.216(2)	2.386(2)	1.880(5)	1.216(8) (CC)	2044	21b
FeCl(CCPh)(dmpe)$_2$	2.218(2)	2.389(1)	1.897(3)	1.192(3) (CC)	2044	21c
$[FeH(N_2)(dmpe)_2](BPh_4)$	2.205(6)	1.32(2) (H)	1.818(11) (N)	1.13(3) (NN)	2094	21b
$FeCl_2(depe)_2$	2.260	2.344(2)				21d
$FeHCl(depe)_2$	2.208	2.404(2) (Cl)				21e
$[FeH(N_2)(depe)_2](BPh_4)$	2.240		1.825(7) (N)	1.1070(12) (NN)	2090	21f
$[FeCl(N_2)(depe)_2](BPh_4)$	2.291(4)	2.311(3)	1.784(9) (N)	1.073(11) (NN)	2088	21g
$[Fe(NCNEt_2)_2(depe)_2](BF_4)_2$	2.279		1.908(8) (N)	1.14(1) (NC)	2225	21h

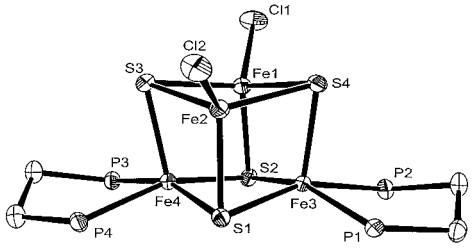

Figure 4. Crystallographic structure of the $Fe_4S_4(depe)_2Cl_2$ (**XI**) cluster.

in **XI** is 2.267(7) Å. The average Fe−P distances for **III**, **VI**, and **VII** are 2.245(8), 2.243(3), and 2.241(4) Å, respectively. Interestingly, the distances of the axial ligands of the square pyramidal Fe centers for Fe(3)−S(4) (2.2859(8) Å) and Fe(4)−S(3) (2.2856(8) Å) in **XI** are significantly longer than those of the other μ_3-S equatorial ligands (Fe(3)−S(1), 2.2624(9) Å; Fe(3)−S(2), 2.2606(8) Å; Fe(4)−S(1), 2.2692(8) Å; Fe(4)−S(2), 2.2522(9) Å). Such a wide range of Fe−S distances also is observed in the structures of the $[Fe_4S_4Cl_4]^{2-}$ and $[Fe_4S_4(SPh)_4]^{2-}$ clusters.[24]

Physical Properties. The infrared spectra of $\{(Cl_4\text{-cat})MoFe_3S_4(depe)_2Cl\}_2(\mu\text{-depe})$ **III** and $\{(Cl_4\text{-cat})MoFe_3S_4(depe)_2\}_2(\mu\text{-S})(\mu\text{-depe})$ **IV** and those of $\{(Cl_4\text{-cat})MoFe_3S_4(dmpe)_2Cl\}_2(\mu\text{-dmpe})$ **V** and $\{(Cl_4\text{-cat})MoFe_3S_4(dmpe)_2\}_2(\mu\text{-S})(\mu\text{-dmpe})$ **VI** were very similar in the 3000−800 cm^{-1} region. The doubly bridged double cubanes **IV** and **VI** show a broad peak at 354 cm^{-1}. Mass spectroscopy (FAB^+ with NBA matrix) shows the compounds **III**, **IV**, **V**, and **VI** fragment into the single cubane units. The isotope distributions of $[(Cl_4\text{-cat})(MoFe_3S_4(depe)_2Cl)_2(depe)]^+$ and $[((Cl_4\text{-cat})MoFe_3S_4(dmpe)_2)_2(dmpe)(S)]^+$ were well matched to those of theoretical expectation. The electronic spectra of compounds **III** and **IV** are shown in Figure 5.

The neutral clusters, **III** and **V**, are singly bridged through the PCH_2CH_2P bridging ligand and have two $[MoFe_3S_4]^{3+}$ subunits in each molecule. Both compounds show an $S = {}^1/_2$ signal in the $g = 2$ region in frozen DMF[25] or CH_2Cl_2 (Figure 6). The compounds in DMF developed new signals upon standing in solution at room temperature. A ligand exchange by DMF molecules and/or structural rearrangements are possible in DMF solution. The $g = 4$ signal for an $S = {}^3/_2$ ground state, characteristic of the $(Et_4N)_2[(Cl_4\text{-cat})Mo(MeCN)Fe_3S_4Cl_3]$ cubane (**I**), is not detected. These results suggest that even though the oxidation state of **III** and **V** has not been changed by ligand substitution, their spin states have changed. The other DBDC's (**IV** and **IV**) showed no EPR signals.

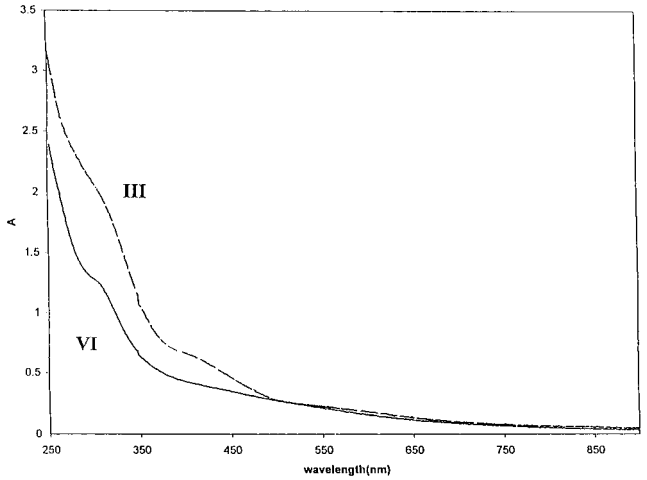

Figure 5. Electronic spectra of the $\{(Cl_4\text{-cat})MoFe_3S_4(depe)_2Cl\}_2(\mu\text{-depe})$ (**III**) and $\{(Cl_4\text{-cat})MoFe_3S_4(dmpe)_2\}_2(\mu\text{-S})(\mu\text{-dmpe})$ (**VI**) clusters in CH_2Cl_2. The broken line represents the absorption spectrum of **III**, and the solid line represents **VI**.

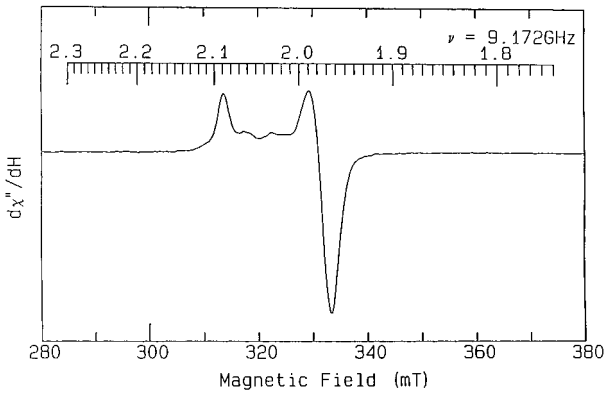

Figure 6. EPR spectrum of the $\{(Cl_4\text{-cat})MoFe_3S_4(depe)_2Cl\}_2(\mu\text{-depe})$ (**III**) cluster in CH_2Cl_2.

Electrochemistry. The results of cyclic voltammetric measurements of the compounds are shown in Table 4. The doubly bridged double cubanes, $\{(Cl_4\text{-cat})MoFe_3S_4(depe)_2\}_2(\mu\text{-S})(\mu\text{-depe})$ (**IV**) and $\{(Cl_4\text{-cat})MoFe_3S_4(dmpe)_2\}_2(\mu\text{-S})(\mu\text{-dmpe})$ (**VI**), show multireduction waves. Because of the very poor solubility of **VI** (even in DMF) and the lack of reliable data, only the results from **IV** will be discussed. In

(25) Compound **I** (140 K): $g = 2.02, 1.92$; $S = {}^1/_2$; signal integration has been done to check the spin/molecule ratio. Compound **II** (74 K): $g = 2.12, 2.09, 2.07, 2.00, 1.98, 1.96$; $S = {}^1/_2$; signal integration has been done to check the concentration.

Table 4. Redox Potential of the Compounds at Room Temperature[a]

compound	$E_{1/2}$, mV	solvent	reference
$(Et_4N)_2[(Cl_4\text{-cat})MoFe_3S_4Cl_3(MeCN)]$ (**I**)	400(rev), −860(rev)	CH_2ClCH_2Cl	9
$(Et_4N)_2[(Cl_4\text{-cat})MoFe_3S_4Cl_3(MeCN)]$ (**I**)	300(rev), −940(rev)	CH_2Cl_2	5b
$(Et_4N)_2[(Cl_4\text{-cat})MoFe_3S_4Cl_3(MeCN)]$ (**I**)	400(rev), −800(rev)	MeCN	12a
$(Cl_4\text{-cat})_2Mo_2Fe_6S_8(Pet_3)_6$ (**II**)	1550(irr), 50(qr), −890(rev), −1450(irr)	CH_2Cl_2	5b
$\{(Cl_4\text{-cat})_2MoFe_3S_4(depe)_2Cl\}_2(\mu\text{-depe})$ (**III**)	820(irr), −153(rev), −947(rev)	CH_2ClCH_2Cl	this work
$\{(Cl_4\text{-cat})_2MoFe_3S_4(depe)_2Cl\}_2(\mu\text{-depe})$ (**III**)	790(irr), −130(rev), −880(rev)	CH_2Cl_2	this work
$\{(Cl_4\text{-cat})_2MoFe_3S_4(depe)_2\}_2(\mu\text{-S})(\mu\text{-depe})$ (**IV**)	520(qr), 260(rev), −155(rev), −645(rev), −955(qr)	CH_2ClCH_2Cl	this work
$\{(Cl_4\text{-cat})_2MoFe_3S_4(dmpe)_2Cl\}_2(\mu\text{-S})(\mu\text{-dmpe})$ (**V**)	687(qr), −94(rev), −869(rev)	CH_2ClCH_2Cl	this work
$\{(Cl_4\text{-cat})_2MoFe_3S_4(dmpe)_2\}_2(\mu\text{-S})(\mu\text{-dmpe})$ (**VI**)	780(rev), 300(rev) −220(rev), −980(rev)	DMF	this work
$(Et_4N)_4\{(Cl_4\text{-cat})MoFe_3S_4Cl_3\}_2(\mu\text{-}N_2H_4)$	320(rev), −900(rev)	CH_2ClCH_2Cl	9
$(Et_4N)_4\{(Cl_4\text{-cat})MoFe_3S_4Cl_3\}_2(\mu\text{-}C_4H_4N_2)$	370(qr), −915(qr)	CH_2ClCH_2Cl	9
$(Et_4N)_4\{(Cl_4\text{-cat})MoFe_3S_4Cl_2\}_2(\mu\text{-S})(\mu\text{-}N_2H_4)$	320(qr), 100(qr) −1060(qr)	MeCN	12a
$(Et_4N)_5\{(Cl_4\text{-cat})MoFe_3S_4Cl_2\}_2(\mu\text{-S})(\mu\text{-OH})$	150(qr), −50(qr) −1200(qr)	CH_2Cl_2	12b
$(Et_4N)_4[(MoFe_3S_4Cl_4)_2(\mu\text{-}C_2O_4)]$	500(qr), −40(qr) −890(qr), −1100(irr)	CH_2Cl_2	8c
$(Et_4N)_3[MoFe_3S_4Cl_4(C_2O_4)]$	500(qr), 250(irr), −1030(irr)	CH_2Cl_2	8c
$(Et_4N)_2[Fe_4S_4(SPh)_4]$ (**VIII**)	−940(rev)	MeCN	this work
$Fe_4S_4(depe)_2(SPh)_2$ (**IX**)	−130(rev), −994(rev)	CH_2ClCH_2Cl	this work
$(Ph_4P)_2[Fe_4S_4(SPh)_2(Et_2dtc)_2]$	−70(qr), −1200(qr)	DMF	23
$(Ph_4P)_2[Fe_4S_4Cl_4]$	−720(rev)	MeCN	26
$(Ph_4P)_2[Fe_4S_4Cl_4]$	−800(rev)	DMF	26
$Fe_4S_4(depe)_2Cl_2$ (**XI**)	130(rev), −58(rev) −875(rev)	CH_2ClCH_2Cl	this work
$(Ph_4P)_2[Fe_4S_4Cl_2(Et_2dtc)_2]$	−205(qr), −1200(rev)	DMF	23a

[a] rev = reversible, irr = irreversible, qr = quasi-reversible

Table 5. Mössbauer Parameters for the Compounds in Zero Applied Magnetic Field

compound	isomer shift, mm/s	quadrupole splitting, mm/s	temp, K	reference
$\{Cl_4\text{-cat})MoFe_3S_4(depe)_2Cl\}_2(\mu\text{-depe})$ (**III**)	0.26 (Fe-depe), 0.36 (1 Fe−Cl)	0.75, 1.01	125	this work
$(Et_4N)_3[(al\text{-cat})MoFe_3S_4(S\text{-}p\text{-}C_6H_4Cl)_4]$	0.30 (2 Fe), 0.30 (1 Fe)	1.18, 1.60	120	29
$(Et_4N)_4[(MoFe_3S_4Cl_4)_2(\mu\text{-}C_2O_4)]$	0.49	0.94	125	8c
$(Et_4N)_4\{(Cl_4\text{-cat})MoFe_3S_4Cl_2\}_2(\mu\text{-S})(\mu\text{-}N_2H_4)$	0.53, 0.51, 0.33	1.17, 0.98, 1.03	125	12a
$(Et_4N)_5\{(Cl_4\text{-cat})MoFe_3S_4Cl_2\}_2(\mu\text{-S})(\mu\text{-CN})$	0.51, 0.49, 0.30	1.23, 0.98, 1.05	125	12a
$(Et_4N)_6\{(Cl_4\text{-cat})MoFe_3S_4Cl_2\}_2(\mu\text{-S})_2$	0.53 (2 Fe), 0.34 (1 Fe)	1.14, 1.13	125	12b
$(Et_4N)_5\{(Cl_4\text{-cat})MoFe_3S_4Cl_2\}_2(\mu\text{-S})(\mu\text{-OH})$	0.53 (2 Fe), 0.34 (1 Fe)	1.19, 1.06	125	12b
$Fe_4S_4(depe)_2(SPh)_2$ (**IX**)	0.38 (2 Fe−SPh), 0.31 (2 Fe-depe)	1.05, 0.71	125	this work
$(Ph_4P)_2[Fe_4S_4(SPh)_4]$	0.43	0.93	77	23a
$(Et_4N)_2[Fe_4S_4Cl_4]$ (**X**)	0.50	1.06	77	30
$(Ph_4P)_2[Fe_4S_4Cl_4]$	0.49	0.67	77	23a
$(Et_4N)_4[(Fe_4S_4Cl_3)_2(\mu\text{-S})]$	0.48	0.98	125	12b
$(Ph_4P)_2[Fe_4S_4(SPh)_2(Et_2dtc)_2]$	0.47 (2 Fe−SPh), 0.64 (2 Fe-Et_2dtc)	1.06, 1.84	77	23a

CH_2ClCH_2Cl, **III** shows two reversible reduction waves at −153 and −947 mV and one irreversible oxidation wave at 820 mV. Under the same conditions, **IV** showed multireduction waves at −155, −645, and −955 mV; the first two reductions are reversible, and the third reduction is quasi-reversible. Two oxidation waves at 520 and 260 mV are quasi-reversible and reversible, respectively. Two reversible reduction waves of **V** at −94 and −869 mV and one quasi-reversible oxidation wave at 687 mV show that the dmpe analogue, compared to **III**, is easier to oxidize and reduce in CH_2ClCH_2Cl. The presence of multiple reduction waves in **IV** suggests that the dimeric structure is retained in solution and the two subunits influence each other electronically. The EPR and cyclic voltammetric data for **III** and **V** do not show significant electronic interactions between the two subunits. The absence of a μ-S^{2-} bridge in both of these clusters and long Mo−Mo distances (>7 Å) apparently hinder mutual electronic interactions (vida infra).

The electronic interactions between the $[MoFe_3S_4]^{3+}$ subclusters of **IV** and **VI**, evident in the lack of an EPR signal and multiple voltammetric waves, most probably are due to the Fe−S−Fe bridges. Similar electronic interactions between two $[MoFe_3S_4]^{3+}$ subunits have been reported before.[11]

Reduction potential measurements for the $Fe_4S_4(depe)_2(SPh)_2$ (**IX**) and $Fe_4S_4(depe)_2Cl_2$ (**XI**) clusters show that the phosphine ligand-substituted single cubanes are easier to reduce than other single cubanes with phenyl thiolate or chloride ligands by 700−900 mV. The comparison between **IX**, **XI**, and **VIII** and $(Ph_4P)_2[Fe_4S_4Cl_4]$[26] shows the general tendency of a single cubane with a chloride ligand to be reduced easier than the one with thiolate ligand by about 100 mV.

Mössbauer Spectroscopy. Mössbauer parameters for the $MoFe_3S_4$ and Fe_4S_4 clusters are shown in Table 5. The Mössbauer spectrum of $\{(Cl_4\text{-cat})MoFe_3S_4(depe)_2Cl\}_2(\mu\text{-depe})$ (**III**) shows a broad quadrupole doublet. The latter was fitted by two Fe centers with $\delta = 0.26$ mm/s and $\Delta E_Q = 0.75$ mm/s, and $\delta = 0.36$ mm/s and $\Delta E_Q = 1.01$ mm/s (2:1 ratio) at 125 K (Figure 7). The average isomer shift of **III** is 0.29 mm/s. The $(Et_4N)_3[Mo_2Fe_6S_8(SR)_9]$ (R = Et, Ph, or CH_2CH_2OH) clusters have three μ-SR^- bridging ligands bound on the Mo sites of the two $[MoFe_3S_4]^{3+}$ subunits. They show isomer shifts of 0.41, 0.42, and 0.41 mm/s at 77 K, respectively.[27] The $[MoFe_3S_4]^{3+}$ single cubane cluster, $(Et_4N)_3[(al\text{-cat})MoFe_3S_4(S\text{-}p\text{-}C_6H_4Cl)_4]$, shows an average isomer

(26) Kanatzidis, M. G.; Baenziger, N. C.; Coucouvanis, D.; Simopoulos, A.; Kostikas, A. *J. Am. Chem. Soc.* **1984**, *106*, 4500.

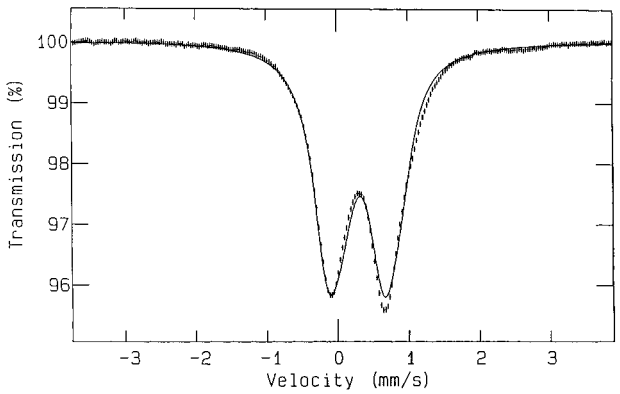

Figure 7. ^{57}Fe Mössbauer spectrum of the $\{(Cl_4\text{-cat})MoFe_3S_4(depe)_2Cl\}_2$-($\mu$-depe) (**III**) cluster measured at 125 K in a zero applied magnetic field. The source was ^{57}Co in a Th matrix, and the isomer shift was reported versus Fe metal at room temperature. The cross marks are for the observed data, and the solid line is the simulation (see text).

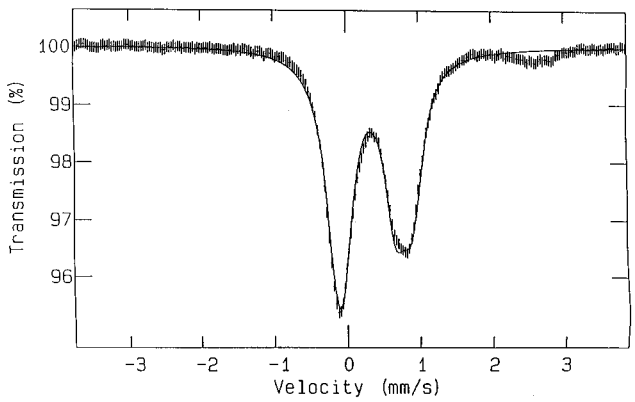

Figure 8. ^{57}Fe Mössbauer spectrum of the $Fe_4S_4(depe)_2(SPh)_2$ (**IX**) cluster measured at 125 K in a zero applied magnetic field. The source was ^{57}Co in a Rh matrix, and the isomer shift was reported versus Fe metal at room temperature. The cross marks are for the observed data, and the solid line is the simulation (see text).

shift of 0.30 mm/s at 120 K.[28] A mean oxidation state of 2.67 for the three Fe atoms in **III** can be obtained from the empirical equation $\delta = 1.44-0.43s$,[29] where δ is isomer shift and s is the mean oxidation state of Fe in the tetrahedral S_4 site.

The Mössbauer spectrum of $Fe_4S_4(depe)_2(SPh)_2$ (**IX**) shows one broad doublet (Figure 8) which was simulated by two different Fe centers ($\delta = 0.38$ and 0.31 mm/s and $\Delta E_Q = 1.05$ and 0.71 mm/s). Two Fe sites are suggested by the coordination environment of the Fe atoms in **IX**. Selected Mössbauer data for related $[Fe_4S_4]^{2+}$ clusters are shown in Table 5. The Ph_4P^+ salt of the **VIII**$^{2-}$ cluster shows an isomer shift of 0.43 mm/s at 77 K.[23] The chloride derivative shows an isomer shift at 0.49 mm/s under the same conditions, and $(Et_4N)_2[Fe_4S_4Cl_4]$ (**X**) shows a doublet at 0.50 mm/s at 77 K (Table 5).[30] The $(Ph_4P)_2[Fe_4S_4(SPh)_2(Et_2dtc)_2]$ cluster shows two isomer shifts of 0.47 and 0.64 mm/s at 77 K.[23a] Introduction of the Et_2dtc^- ligands increased the isomer shift in the latter, and the pentacoordinate square pyramidal Fe centers with Et_2dtc^- as terminal ligands give rise to the doublet with $\delta = 0.67$ mm/s and $\Delta E_Q = 1.84$. The isomer shift and quadrupole splitting of the tetrahedral Fe centers with SPh terminal ligands in the $(Ph_4P)_2[Fe_4S_4(SPh)_2(Et_2dtc)_2]$ cluster have increased from those of the same Fe centers in the $(Ph_4P)_2[Fe_4S_4(SPh)_4]$ cluster. The former are $\delta = 0.47$ mm/s and $\Delta E_Q = 1.06$ mm/s, and the latter are $\delta = 0.43$ mm/s and $\Delta E_Q = 0.93$ mm/s.

In the core of **IX**, two Fe(II) and two Fe(III) centers have been assigned on the basis of the ligands and the coordination geometry. The square pyramidal Fe centers with coordinated depe ligands are assigned as Fe(II) sites, and the tetrahedral Fe centers with phenylthiolate ligand are assigned as Fe(III) sites. The latter gives rise to the doublet at $\delta = 0.38$ mm/s and $\Delta E_Q = 1.05$ mm/s, and the former gives rise to the doublet at $\delta = 0.31$ mm/s and $\Delta E_Q = 0.71$ mm/s (Figure 8). For **III** and **IX**, respectively ($Fe^{+2.67}$ and $Fe^{+2.50}$ clusters), the Fe centers with Cl^- or SPh^- ligands were assigned the doublets at $\delta = 0.36$ mm/s or $\delta = 0.38$ mm/s. The Fe centers with coordinated depe ligands were assigned the doublets at $\delta = 0.26$ mm/s and $\delta = 0.31$ mm/s.

Acknowledgment. The authors acknowledge the support of this work by a grant from the National Institutes of Health (GM 33080). Dr. Namdoo Moon in the Biophysics Department at The University of Michigan is greatly appreciated for his Mössbauer and EPR measurements and helpful discussion.

Supporting Information Available: X-ray crystallographic files in CIF format for the structure determinations of **III**, **VI**, **VII**, and **XI**. These materials are available free of charge via the Internet at http://pubs.asc.org.

IC010913+

(27) Christou, G.; Garner, C. D.; Miller, R. M. *J. Chem. Soc., Dalton Trans.* **1980**, 2363.
(28) (a) al-cat = 3,6-diallylcatecholate. (b) Mascharak, P. K.; Papaethymiou, G. C.; Armstrong, W. H.; Foner, S.; Frankel, R. B.; Holm, R. H. *Inorg. Chem.* **1983**, *22*, 2851.
(29) Christou, G.; Mascharak, P. K.; Armstrong, W. H.; Papaethymiou, G. C.; Frankel, R. B.; Holm, R. H. *J. Am. Chem. Soc.* **1982**, *104*, 2820.
(30) Evans, D. J.; Hills, A.; Hughes, D. L.; Leigh, G. J. *J. Chem. Soc., Dalton Trans.* **1990**, 2735.